

# Josephson oscillations of edge quasi-solitons in a photonic-topological coupler

NATALIIA BAZHAN<sup>1,\*</sup>, BORIS MALOMED<sup>2,3</sup>, AND ALEXANDER YAKIMENKO<sup>1</sup>

<sup>1</sup>Department of Physics, Taras Shevchenko National University of Kyiv, 64/13, Volodymyrska Street, Kyiv 01601, Ukraine

<sup>2</sup>Department of Physical Electronics, Faculty of Engineering, and Center for Light-Matter Interaction, Tel Aviv University, Tel Aviv 69978, Israel

<sup>3</sup>Instituto de Alta Investigación, Universidad de Tarapacá, Casilla 7D, Arica, Chile

\*Corresponding author: nataliia.bazhan@gmail.com

Compiled November 30, 2021

We introduce a scheme of a photonic coupler built of two parallel topological-insulator slab waveguides with the intrinsic Kerr nonlinearity, separated by a lattice spacing. Josephson oscillations (JO) of a single edge quasi-soliton (QS) created in one slab, and of a pair of Qs created in two slabs, are considered. The single QS jumping between the slabs is subject to quick radiative decay. On the other hand, the JO of the copropagating QS pair may be essentially more robust, as one QS absorbs dispersive waves emitted by the other. The most robust JO regime is featured by the pair of Qs with phase shift  $\pi$  between them. © 2021

Optical Society of America

<http://dx.doi.org/10.1364/ao.XX.XXXXXX>

Topological insulators (TIs) are materials that are insulating in a bulk but conducting at the surface, due to the existence of scattering-resistant topological edge states. Recently, it was discovered that the topological phases are not restricted to solid-state fermionic states, but can also be realized in photonic crystals and metamaterials [1–6]. Rapidly growing interest in topological effects in photonics is motivated by possibilities to design light-guiding and routing photonic circuits in a manner that is stable against disorder, due to the robustness of topological edge states. Developing these studies, solitons have been recently observed in the bulk of a photonic Floquet TI [7], and theoretically elaborated in other TI setups [8–10]. They exhibit dynamics different from that demonstrated by solitons in ordinary bandgap settings [11], *viz.*, cyclotron-like orbits induced by the photonic-lattice topology. The concept of topological lasers based on the Floquet TI was put forward in [12]. It is based on a truncated array of lasing helical waveguides, with the pseudo-magnetic field induced by their twist along the propagation direction, opening up a topological lattice gap by breaking the time-reversal symmetry. Localized edge states in a similar system were analyzed too [13]. Further, the recent study [14] dealt with topological edge states maintained by a domain wall between two helical honeycomb lattices with opposite helicities. In that system, nonlinearity helps to create robust edge states in the form of fundamental and multipole solitons, including moving ones.

In this work, we address interactions between nonlinear topological surface wave packets copropagating along opposite edges of two slab-shaped TI waveguides separated by free space. The setup, displayed in Fig. 1, is a *coupler*, *i.e.*, a set of two parallel waveguides with an empty space between them, which are *coupled* by tunneling of the field. Oscillatory dynamics of wave modes in the coupler is usually categorized as *Josephson oscillations* (JO) [15]. Long Josephson junctions [16] were the first well-studied example of nonlinear couplers for wave modes (fluxons in bulk superconductors separated by a narrow dielectric barrier). Various realizations of couplers are also known in optics [17] and Bose-Einstein condensates [18–21]. The present work aims to elaborate the scheme of the *photonic TI coupler* and analyze the dynamics of composite nonlinear modes in it. In this connection, it is relevant to mention a recently elaborated scheme for resonant coupling between excitations on opposite edges of a single TI slab [22].

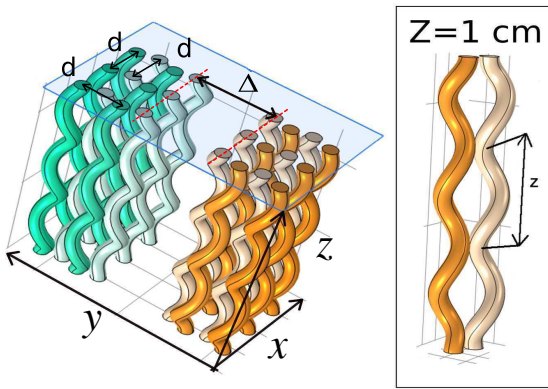
The photonic structure of each waveguiding slab building the coupler is similar to that proposed in Refs. [23, 24] for the creation of surface solitons in the semi-infinite bulk waveguide. The band structure of a single-slab lattice is similar to the band structure of anomalous Floquet TIs investigated in [23]. The 2D Floquet TI maintains protected edge states even if all bands have zero Chern number [25–28]. Our consideration reveals the propagation of nonlinear wave packets at the edge of the lattice, in agreement with the topological structure of the underlying linear band structure described in [24]. In the paraxial approximation, the propagation of the optical-beam envelope  $\psi(x, y, z)$  along coordinate  $z$  obeys the nonlinear Schrödinger equation (NLSE),

$$i\partial_z\psi = -(2k_0)^{-1}\nabla_{\perp}^2\psi - k_0n_0^{-1}(n_L(x, y, z) + n_2|\psi|^2)\psi, \quad (1)$$

with the diffraction operator,  $\nabla_{\perp}^2 \equiv \partial_x^2 + \partial_y^2$ , acting on transverse coordinates  $(x, y)$ . Here  $k_0 = 2\pi n_0/\lambda$  is the wavenumber corresponding to the carrier wavelength  $\lambda$ ,  $n_0$  is the background refractive index,  $n_2|\psi|^2$  is the nonlinear correction to it, and  $n_L(x, y, z)$  represents the helix-lattice background [29] with helix radius  $R_0$ , lattice spacing  $a$ , and modulation period  $Z$ . We adopt parameters consistent with fused silica glass at  $\lambda = 1.55 \mu\text{m}$ :  $n_0 = 1.45$ ,  $n_L = 2.7 \times 10^{-3}$  in the waveguides (and  $n_L = 0$  outside), and  $n_2 = 3 \times 10^{-7} \text{ cm}^2/\text{GW}$  [30]. Individual helices have the circular cross section with  $R_0 = 4 \mu\text{m}$ .

The beam intensity  $|\psi|^2$  is normalized by a characteristic value  $I_0 = 10^3 \text{ GW/cm}^2$ , for which the nonlinear index shift  $n_2 I_0$  is comparable to  $n_L$ . For the modal cross-section area of the helix  $w_0^2 = (10 \mu\text{m})^2$ , this  $I_0$  corresponds to peak powers  $\sim 1 \text{ MW}$ , readily accessible with pulsed lasers [30]. Here we do not consider temporal effects, which is a subject for a separate work.

**Fig. 1.** A sketch of two photonic lattices composed of helical waveguides. The lattices are separated by the spacing of width  $\Delta$ . One lattice consists of (green) waveguides twisted clockwise, while the other (orange) lattice is the mirror reflection of the green one relative to the midplane of the lattice spacing. This setup allows copropagation of two QSs (quasi-solitons) on opposite edges of the lattice spacing. The waveguides in each lattice are shifted relative to each other along the  $z$ -axis by half of the modulation period,  $Z = 1 \text{ cm}$ . Shown are the lattices composed of  $n_y^s = 4$  shells ( $n_y = 2$ ).



In this work we consider a coupler composed of two mirror-symmetric staggered helical lattices separated by a gap of width  $\Delta$ , as shown in Fig. 1. Due to opposite signs of the twist of the waveguides in the lattices, two edge nonlinear wave packets copropagate in the same direction along the edges of the lattices, and interact with each other across the spacing. For each lattice we use parameters of nonlinear photonic Floquet TIs introduced in [23, 24]. The lattices consist of 2D square arrays of helical waveguides, *staggered* so that adjacent waveguides have helix phase shifts of  $\pi$  relative to each other, as shown in the right panel of Fig. 1. Note that, while  $z$  varies within one period  $Z$ , each waveguide is approaching its four neighbors sequentially. The respective modulation of the linear refractive index in Eq. (1), which describes the coupler shown in Fig. 1, is adopted as

$$n_L(x, y, z) = \Delta n_1 \sum_{n=-[n_x/2]}^{[n_x/2]} \sum_{m=1}^{n_y} \left\{ V_0(x - X_n^-, y \mp Y_{m-1}^\pm) + V_0(x - X_{n-1/2}^+, y \mp Y_{m-1/2}^\pm) \right\}, \quad (2)$$

where  $n_x$  and  $n_y$  are numbers of shells, equal in both lattices (accordingly, total numbers of waveguiding rows and columns in each slab are  $n_{y,x}^s = 2n_{y,x}$ ). We build the coupler starting from its center. Thus, we summation in Eq. (2) includes all waveguides along the  $x$  axis in the range of  $\{-[n_x/2], +[n_x/2]\}$ , where  $[...]$  stands for the integer part. Both slabs include  $n_y$  shells, factors  $V_0(y - Y_m^+)$  and  $V_0(y + Y_m^-)$  pertaining to the top and bottom slabs. Further, functions introduced in Eq. (2) are

$$X_n^\pm(z) = nd \pm x_0(z), \quad Y_m^\pm(z) = \Delta/2 + md \pm y_0(z). \quad (3)$$

Here,  $\Delta n_1 = 2.7 \times 10^{-3}$  is the modulation depth,  $d = \sqrt{2}a$  is the lattice constant and  $\Delta$  the spacing width in Fig. 1.

We assume a hypergaussian waveguide's profiles in Eq. (2), viz.,

$$V_0(x, y) = \exp\left(-[(x^2 + y^2)/\sigma^2]^3\right), \quad (4)$$

with  $\sigma = 4 \mu\text{m}$ . The waveguides' axes are shaped as helices,

$$x_0(z) = R_0 \cos(\Omega z), \quad y_0(z) = R_0 \sin(\Omega z), \quad (5)$$

with radius  $R_0 = 4 \mu\text{m}$  and pitch  $Z = 2\pi/\Omega = 1 \text{ cm}$ . These parameters are chosen to provide a balance between the minimization of bending losses, which inevitably accompany the nearest-neighbor couplings in the present setting, and the necessity to fit sufficiently many helix cycles to an experimentally feasible total array length,  $\lesssim 10 \text{ cm}$ .

Our objective is to explore the interaction between two wave packets copropagating along edges of the slab-shaped lattice waveguides forming the coupler in Fig. 1. We consider the nonlinear edge packets as "quasi-solitons" (QSs), as they keep soliton-like shapes, while radiating power at a small rate [7]. As shown by Fig. 2, the QSs move in the same direction due to the mutual mirror symmetry of the parallel slabs. The interaction between them is mediated by electromagnetic field traversing the spacing between the slabs.

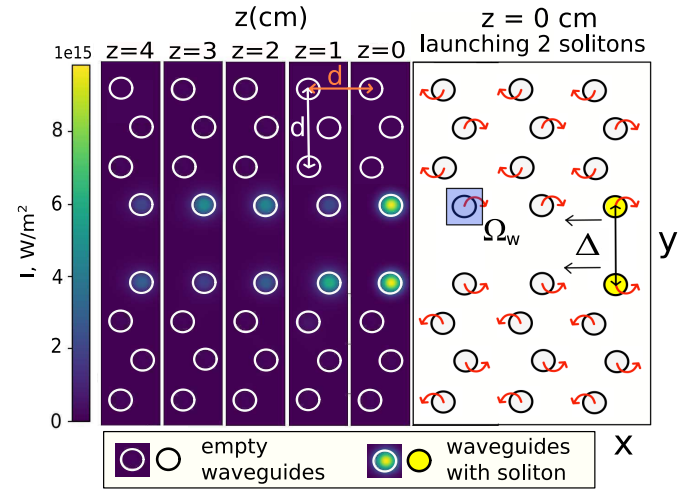


**Fig. 2.** Configurations of the copropagating QSs in the dual-waveguide coupler in the  $(x, y)$  cross-section at different values of propagation distance  $z$ . The QSs are launched at  $z = 0$ , and subsequent configurations, produced by the numerical solution of Eq. (1), are displayed at  $z = 1, 2, 3, 4 \text{ cm}$ . The distance between waveguides in each lattice is  $d \approx 31 \mu\text{m}$ . The spacing between the lattices,  $\Delta$ , is the same as in Eq. (3). Circles indicate cross-sections of individual waveguides and arrows designate the direction of their twist. See Visualization 1 in the Supplement as an example.

First, we produce individual edge QS solutions of NLSE (1) with the effective potential defined as per Eqs. (2)-(5), starting from input

$$\Psi(x, y; z = 0) = \sqrt{I} \exp(-(\mathbf{r} - \mathbf{r}_0)^2/2a^2), \quad (6)$$

where  $\mathbf{r}_0$  is the initial position of the QS, and  $I$  is its peak power. The edge QS, while it can pass a considerable distance, is not a completely stable object, being subject, as mentioned above,

to losses due to emission of small-amplitude dispersive waves [23], see Fig. 3. The loss rate depends on number  $n_y$  of layers in the lattice slab in the direction across the lattice, see Fig. 3. To find an optimal value of  $n_y$ , we computed the power of a single QS propagating along the edge of one slab. The results, displayed in the top plot of Fig. 3, demonstrate that the edge QS traveling in a thin slab, with  $n_y \leq 3$ , decays faster than in the thicker one, with  $n_y \geq 4$ . Therefore, we ran the systematic numerical analysis using the slabs with  $n_y = 4$ . Then, Fig. 3 shows that the peak power of the QS decreases by  $\simeq 10$  times, having passed 10 cm in the  $z$  direction. Because the QS moves along the  $z$  axis in the lattice with pitch  $Z = 1$  cm, it shifts by 10 helix waveguides in the  $x$  direction while passing 10 cm along  $z$ . This means that one needs to have the number of layers  $n_x \geq 10$  in the slab along  $x$ . In the simulations, we used the lattices with  $n_x = 18$ . Animations of QSs propagating on the opposite edges of the coupler are presented in Supplemental Material.

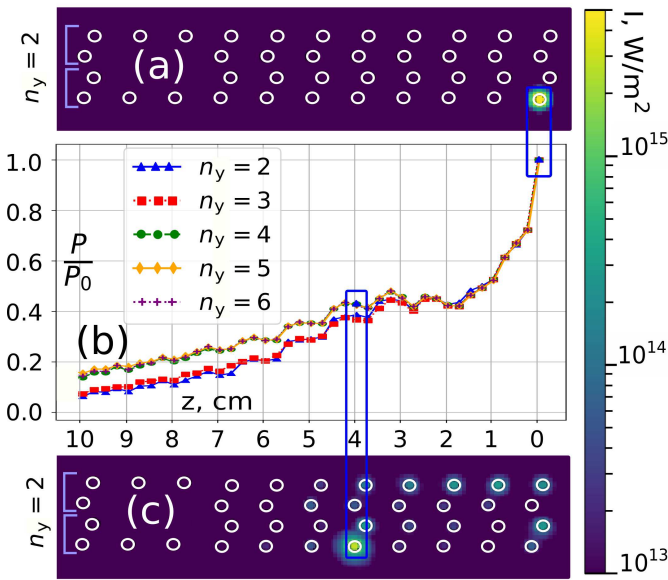


**Fig. 3.** The single edge QS traveling from right to left in the lattice slab built of  $n_y$  layers. In (a) and (c) yellow circles show the location of the QS at  $z = 0$  and  $z = 4$  cm, respectively. The logarithmic color bar on the right indicates the intensity. White circles indicate cross-sections of individual helix waveguides. In (c), the energy lost by the quasi-soliton spreads along the lattice waveguides. (b) The evolution of the peak power of the QS.

To address the interaction of two edge QSs carried by the parallel slabs in the coupler, as shown in Fig 2, we assume that they move with equal velocities, which maximizes the impact of the interaction. Generally, the interaction effects are transient ones because, as mentioned above, each QS in isolation loses 90% of its energy after passing the distance  $z = 10$  cm. The dominant mechanism of the losses is the diffraction of the wave packet, while bending losses are very low [23, 24]. It is well known that the interaction between solitons depends on their peak powers, distance, and relative phase,  $\Delta\phi$  [31]. We monitored the evolution of  $\Delta\phi(z) = \phi_{top} - \phi_{bott}$  and the power difference between the edge QSs maintained by the top and bottom slabs,  $\Delta P(z) = \int_{\Sigma} [|\psi_{top}(x, y, z)|^2 - |\psi_{bott}(x, y, z)|^2] dx dy$ , where  $\Sigma$  is the biggest area around the given helical waveguide which

does not touch adjacent ones, see the right panel of Fig. 2), while  $\phi_{top}$  and  $\phi_{bott}$  are the phases measured at centers of the waveguides.

The power distribution in the interacting QSs depends on spacing  $\Delta$ , the initial value of  $\Delta\phi$ , and the initial power (taken equal for both solitons). As the result of the interaction, an essential part of the QSs' energy oscillates between the slabs, realizing the JO with the frequency which depends on  $\Delta$  and  $\Delta\phi$ . Josephson oscillations are observable only between close enough slabs.

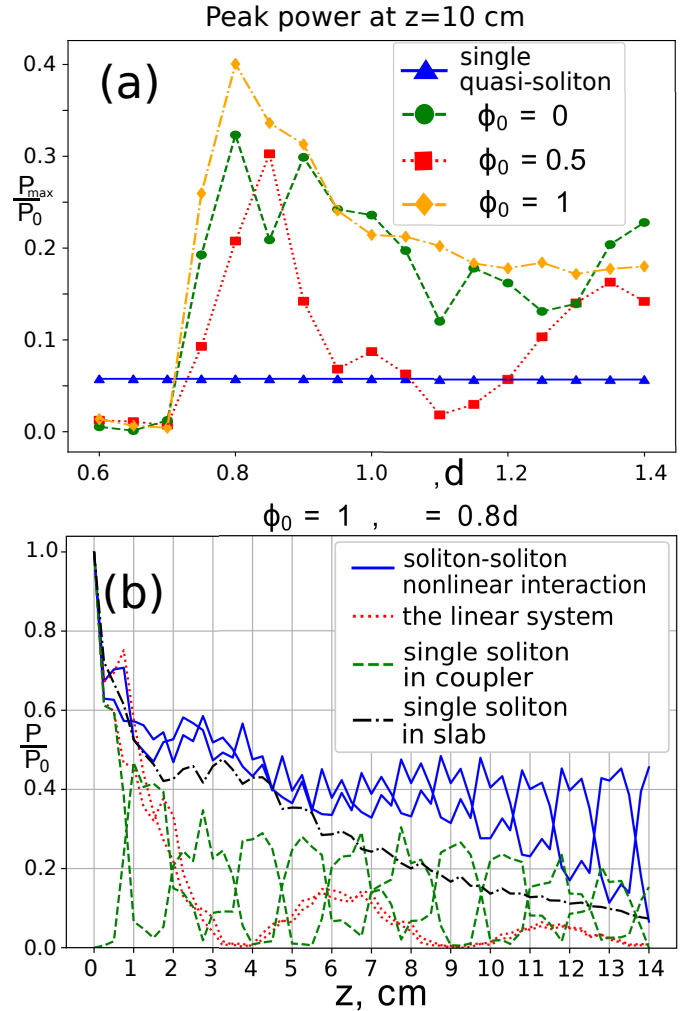


**Fig. 4.** (a) The peak power (normalized to  $P_0$ , see Eq. (6)) of the single QS and QS pair, with different phase shifts, after having passed distance  $z = 10$  cm, vs. the spacing between the parallel waveguiding slabs. (b) The peak power of the single QS, and largest powers of the QS pair in the top and bottom slabs, vs. the propagation distance, for the coupler with spacing  $\Delta = 0.8d$  and phase shift of the pair  $\Delta\phi(0) = \pi$  (it is the optimal set of parameters for the realization of the JO by the pair, according to panel (a)). Also displayed is the decay of the same initial pair of pulses as the QS, but in the linear system. See Visualizations 1-4 in the Supplement illustrating the graph curves.

A significant result produced by systematic simulations of the JO is that the two-QS configuration is essentially *less vulnerable* to the decay than the single edge QS. This trend is ex-

plained by the fact that dispersive waves emitted by one QS are absorbed by the other. Accordingly, in the two-QS dynamical regimes the energy stays concentrated in the QSs, making them brighter.

In Fig. 4(a), the peak power of the single- and two-QS configurations is displayed as a function of the spacing,  $\Delta$ , in the state produced by the simulations at  $z = 10$  cm. It is seen that the strong interaction across the narrow spacing, with  $\Delta \leq 0.75d$ , leads to fast decay of the QSs, faster than the single QS loses its energy. However, at  $\Delta = 0.80d$ , the interaction gives a significant boost to the QS's robustness for all initial phase shifts, the largest boost being observed for  $\Delta\phi(0) = \pi$ . The latter finding is natural, as the repulsion between the QSs helps to suppress their decay.

In Fig. 4(b) we compare the results produced by the propagation of the single edge QS on a separate slab, JO of a single edge QS in the coupler, and the pair of QSs with  $\Delta\phi(0) = \pi$  in the coupler with  $\Delta = 0.80d$  (the latter configuration provides the most robust QSs). The results, represented by the dependence of the peak power on the propagation distance,  $z$ , clearly demonstrate that the interaction between the QSs indeed helps to stabilize them, due to the mutual absorption of the dispersive waves emitted by each one. For the comparison's sake, Fig. 4(b) also displays very fast decay of the same pair of pulses as the initial QSs, but in the linear system. In Supplemental Material we provide videos of the system's evolution for cases illustrated in Fig. 4(b), as well as other details of the JO dynamics.

The topology of the coupler plays a key role in protecting the edge QSs from decay when passing the defects. It can be demonstrated (see details in Supplement) that missing edge waveguides or even the absence of extended segments of the edge lattice does not destroy the coupled evolution of the QSs pair (see Visualizations 5, 7-10 in the Supplement). On the other hand, a missing waveguide near the edge of the single slab causes decay of a QS passing the defect (see Visualization 2). The only situation in which the QSs remain robust in the presence of the defect is when they jump over it due to JO in the two-slab coupler (see Visualizations 7-13).

In conclusion, we have analyzed the dynamics of the single edge QS (quasi-soliton) and a pair of QSs copropagating in the coupler built of parallel photonic TIs (topological insulators) separated by space. The single QS performs JO (Josephson oscillations) between the parallel waveguides, quickly losing energy through the emission of radiation. The evolution of the QS pair demonstrates essentially more robust dynamics, as dispersive waves emitted by one QS are absorbed by the other, in the course of their coupled JO. The two-QS dynamics depends on the phase shift  $\Delta\phi(0)$  between the QSs, the most robust regime corresponding to  $\Delta\phi(0) = \pi$ , in which case they periodically bounce back from each other. As an extension of the analysis, it may be interesting to consider a circular cavity, in the form of the photonic TI (topological-insulator) coupler closed into a ring. The JO of the QSs running along the ring may be additionally stabilized by external gain.

**Acknowledgments.** The authors thank O. G. Chelpanova and V. R. Tuz for fruitful discussions.

**Funding.** The work of B.A.M. was supported, in part, by the Israel Science Foundation, through grant No. 1286/17. NB and AY acknowledge support from National Research Foundation of Ukraine, through grant No. 2020.02/0032.

**Disclosures.** The authors declare no conflicts of interest.  
**Data availability.** No data were generated or analyzed in the presented research.

See Supplement 1 for supporting content.

## REFERENCES

1. S. M. Lu Ling, Joannopoulos John D., Nat. Photonics **8**, 821 (2014).
2. T. Ozawa, H. M. Price, A. Amo, N. Goldman, M. Hafezi, L. Lu, M. C. Rechtsman, D. Schuster, J. Simon, O. Zilberberg, and I. Carusotto, Rev. Mod. Phys. **91**, 015006 (2019).
3. D. Smirnova, D. Leykam, Y. Chong, and Y. Kivshar, Appl. Phys. **7**, 021306 (2020).
4. R. J. Kim Minkyung, Jacob Zubin, Light. Sci. Appl. **9**, 130 (2020).
5. M. Kremer, L. J. Maczewsky, M. Heinrich, and A. Szameit, Opt. Mater. Express **11**, 1014 (2021).
6. D. D. Solnyshkov, G. Malpuech, P. St-Jean, S. Ravets, J. Bloch, and A. Amo, Opt. Mater. Express **11**, 1119 (2021).
7. S. Mukherjee and M. C. Rechtsman, Conf. on Lasers Electro-Optics p. FTh4H.6 (2020).
8. S. K. Ivanov, Y. V. Kartashov, L. J. Maczewsky, A. Szameit, and V. V. Konotop, Opt. Lett. **45**, 1459 (2020).
9. S. K. Ivanov, Y. V. Kartashov, L. J. Maczewsky, A. Szameit, and V. V. Konotop, Opt. Lett. **45**, 2271 (2020).
10. S. K. Ivanov, Y. V. Kartashov, M. Heinrich, A. Szameit, L. Torner, and V. V. Konotop, Phys. Rev. A **103**, 053507 (2021).
11. Y. S. Kivshar and G. P. Agrawal, *Optical Solitons: From Fibers to Photonic Crystals* (2003).
12. S. K. Ivanov, Y. Zhang, Y. V. Kartashov, and D. V. Skryabin, APL Photonics **4**, 126101 (2019).
13. M. J. Ablowitz, C. W. Curtis, and Y.-P. Ma, Phys. Rev. A **90**, 023813 (2014).
14. Z. Shi, M. Zuo, H. Li, D. Preece, Y. Zhang, and Z. Chen, ACS Photonics **8**, 1077 (2021).
15. B. A. Malomed, *Spontaneous Symmetry Breaking, Self-Trapping, and Josephson Oscillations* (Springer-Verlag: Berlin and Heidelberg, 2013).
16. A. V. Ustinov, *Solitons in Josephson Junctions: Physics of Magnetic Fluxons in Superconducting Junctions and Arrays* (Pearson, New York, 2015).
17. B. A. Malomed, "A variety of dynamical settings in dual-core nonlinear fibers", In: *Handbook of Optical Fibers*, vol. 1 (G.-D. Peng, Editor: Springer, Singapore, 2019, 2019).
18. I. Bloch, T. W. Hänsch, and T. Esslinger, Phys. Rev. Lett. **82**, 3008 (1999).
19. S. Raghavan, A. Smerzi, S. Fantoni, and S. R. Shenoy, Phys. Rev. A **59**, 620 (1999).
20. M. Albiez, R. Gati, J. Fölling, S. Hunsmann, M. Cristiani, and M. K. Oberthaler, Phys. Rev. Lett. **95**, 010402 (2005).
21. Z. Chen, Y. Li, and B. A. Malomed, Phys. Rev. Res. **2**, 033214 (2020).
22. Y. Zhang, Y. V. Kartashov, Y. Zhang, L. Torner, and D. V. Skryabin, Laser & Photonics Rev. **12**, 1700348 (2018).
23. D. Leykam and Y. D. Chong, Phys. Rev. Lett. **117**, 143901 (2016).
24. D. Leykam, M. C. Rechtsman, and Y. D. Chong, Phys. Rev. Lett. **117**, 013902 (2016).
25. T. Kitagawa, E. Berg, M. Rudner, and E. Demler, Phys. Rev. B **82**, 235114 (2010).
26. M. S. Rudner, N. H. Lindner, E. Berg, and M. Levin, Phys. Rev. X **3**, 031005 (2013).
27. P. Titum, N. H. Lindner, M. C. Rechtsman, and G. Refael, Phys. Rev. Lett. **114**, 056801 (2015).
28. D. Carpentier, P. Delplace, M. Fruchart, and K. Gawędzki, Phys. Rev. Lett. **114**, 106806 (2015).
29. Z. Shi, D. Preece, C. Zhang, Y. Xiang, and Z. Chen, Opt. Express **27**, 121 (2019).
30. A. Szameit, J. Burghoff, T. Pertsch, S. Nolte, A. Tünnermann, and F. Lederer, Opt. Express **14**, 6055 (2006).
31. Y. S. Kivshar and B. A. Malomed, Rev. Mod. Phys. **61**, 763 (1989).

1. Soljaci Marin Lu Ling Joannopoulos John D. "Topological photonics". *Nature Photonics*8.11 (Nov. 2014), pp. 821–829.
2. Tomoki Ozawa et al. "Topological photonics". *Rev. Mod. Phys.*91(1 Mar. 2019), p. 015006.
3. Daria Smirnova et al. "Nonlinear topological photonics". *Appl. Phys.*7 (2020), p. 021306.
4. Rho Junsuk Kim Minkyung Jacob Zubin. "Recent advances in 2D,3D and higher-order topological photonics". *Light: Science and Applications*9 (July 2020), p. 130.
5. Mark Kremer et al. "Topological effects in integrated photonic waveguide structures". *Opt. Mater. Express*11.4 (Apr. 2021), pp. 1014–1036.
6. Dmitry D. Solnyshkov et al. "Microcavity polaritons for topological photonics". *Opt. Mater. Express*11.4 (Apr. 2021), pp. 1119–1142.
7. Seababrata Mukherjee and Mikael C. Rechtsman. "Observation of Topological Band Gap Solitons". *Science*368 (2020), pp. 856–859.
8. Sergey K. Ivanov and Yaroslav V. Kartashov and Lukas J. Maczewsky and Alexander Szameit and Vladimir V. Konotop. "Edge solitons in Lieb topological Floquet insulator". *Opt. Lett.* (Mar. 2020).
9. S. K. Ivanov and Y. V. Kartashov and L. J. Maczewsky and A. Szameit and V. V. Konotop. "Bragg solitons in topological Floquet insulators". *Opt. Lett.* (Apr. 2020).
10. Ivanov, Sergey K. and Kartashov, Yaroslav V. and Heinrich, Matthias and Szameit, Alexander and Torner, Lluís and Konotop, Vladimir V. "Topological dipole Floquet solitons". *Phys. Rev. A*, 2021.
11. Y S. Kivshar and G P. Agrawal. "Optical Solitons: From Fibers to Photonic Crystals". Academic Press(2003).
12. Sergey K. Ivanov et al. "Floquet topological insulator laser". *APL Photonics*4 (2019), p. 126101.
13. Ablowitz, Mark J. and Curtis, Christopher W. and Ma, Yi-Ping. "Linear and nonlinear traveling edge waves in optical honeycomb lattices". *Phys. Rev. A* (Aug. 2014), p. 023813.
14. Zhiwei Shi et al. "Topological Edge States and Solitons on a Dynamically Tunable Domain Wall of Two Opposing Helical Waveguide Arrays". *ACS Photonics*8.4 (2021), pp. 1077–1084.
15. B. A. Malomed. "Spontaneous Symmetry Breaking, Self-Trapping, and Josephson Oscillations". Springer-Verlag: Berlin and Heidelberg, 2013.
16. A. V. Ustinov. "Solitons in Josephson Junctions: Physics of Magnetic Fluxons in Superconducting Junctions and Arrays". Pearson, New York, 2015.
17. B. A. Malomed. "A variety of dynamical settings in dual-core nonlinear fibers", *Handbook of Optical Fibers*. Vol. 1. G.-D. Peng, Editor : Springer, Singapore, 2019, pp. 421–474.
18. Immanuel Bloch, Theodor W. Hänsch, and Tilman Esslinger. "Atom Laser with a cw Output Coupler". *Phys. Rev. Lett.*82 (Apr. 1999), pp. 3008–3011.
19. S. Raghavan et al. "Coherent oscillations between two weakly coupled Bose-Einstein condensates: Josephson effects,  $\pi$ -oscillations, and macroscopic quantum self-trapping". *Phys. Rev. A*59 (Jan. 1999), pp. 620–633.
20. Michael Albiez et al. "Direct Observation of Tunneling and Nonlinear Self-Trapping in a Single Bosonic Josephson Junction". *Phys. Rev. Lett.*95 (June 2005), p. 010402.
21. Zhaopin Chen, Yongyao Li, and Boris A. Malomed. "Josephson oscillations of chirality and identity in two-dimensional solitons in spin-orbit coupled condensates". *Phys. Rev. Research*2 (Aug. 2020), p. 033214.
22. Zhang, Yiqi and Kartashov, Yaroslav V. and Zhang, Yanpeng and Torner, Lluís and Skryabin, Dmitry V. "Resonant Edge-State Switching in Polariton Topological Insulators". *Laser & Photonics Reviews*, 2018.
23. Daniel Leykam and Y. D. Chong. "Edge Solitons in Nonlinear Photonic Topological Insulators". *Phys. Rev. Lett.*117 (14 Sept. 2016), p. 143901.
24. Daniel Leykam, M. C. Rechtsman, and Y. D. Chong. "Anomalous Topological Phases and Unpaired Dirac Cones in Photonic Floquet Topological Insulators". *Phys. Rev. Lett.*117 (1 June 2016), p. 013902.
25. Kitagawa, Takuya and Berg, Erez and Rudner, Mark and Demler, Eugene. "Topological characterization of periodically driven quantum systems". *Phys. Rev. B* (Dec. 2010), p. 235114.
26. Rudner, Mark S. and Lindner, Netanel H. and Berg, Erez and Levin, Michael. "Anomalous Edge States and the Bulk-Edge Correspondence for Periodically Driven Two-Dimensional Systems". *Phys. Rev. X* (Jul, 2013), p.031005.
27. Titum, Paraj and Lindner, Netanel H. and Rechtsman, Mikael C. and Refael, Gil. "Disorder-Induced Floquet Topological Insulators". *Phys. Rev. Lett.* (Feb, 2015), p. 056801
28. Carpentier, David and Delplace, Pierre and Fruchart, Michel and Gawedzki, Krzysztof. "Topological Index for Periodically Driven Time-Reversal Invariant 2D Systems". *Phys. Rev. Lett.* (Mar, 2015), p.106806.
29. Zhiwei Shi et al. "Generation and probing of 3D helical lattices with tunable helix pitch and interface". *Optics Express*27.1 (Jan. 2019), p. 121.
30. Alexander Szameit et al. "Two-dimensional soliton in cubic fs laser written waveguide arrays in fused silica". *In: Optics Express*14.13 (June 2006), pp. 6055–6062.
31. Yuri S. Kivshar and Boris A. Malomed. "Dynamics of solitons in nearly integrable systems". *In: Rev. Mod. Phys.*61 (Oct. 1989), pp. 763–915.